Electronic Supplementary Material (ESI) for Journal of Materials Chemistry A.

Supplementary Information

Shape-controlled Mesoporous Melamine-formaldehyde Polymers by Solvent-assisted Curing

Inah Kang[1], Young Rok Yoon[1], Seul Ah Lee[1], Seong Jong Kim[1] and Sang Youl Kim[*1]

[1] Department of Chemistry, Korea Advanced Institute of Science and Technology (KAIST), Daejeon *34141*, Republic of Korea.

[*] Correspondence to S. Y. Kim (E-mail: kimsy@kaist.ac.kr)

Experimental Section

Materials. Melamine, paraformaldehyde, 6-chloro-1,3,5-triazine-2,4-diamine, ethylene diamine, piperazine, triethylamine, formaldehyde solution (37 wt. % in H_2O, contains 10-15% methanol as stabilizer), Span® 80 and sulfolane were purchased from Sigma-Aldrich. Sodium hydroxide, hydrochloric acid, cyclohexane and dimethyl sulfoxide (DMSO) were purchased from Daejung. Dimethylacetamide (DMAc), dimethylformamide (DMF), 1-*N*-methyl-2-pyrrolidone (NMP), ethylene acetate, tetrahydrofuran and acetonitrile were purchased from Junsei. All reactants were used without further purification.

Characterization. Fourier transform infrared spectroscopy (FT-IR) spectra were recorded on a Thermo Fisher Scientific Nicolet iS50. Optical microscope (OM) images were obtained on Nikon Eclipse ME600 and field emission scanning electron microscope (FE-SEM) images were obtained on Hitachi SU5000. ^1H and ^{13}C nuclear magnetic resonance (NMR) spectra of synthesized materials were recorded on an Agilent Technologies DD2 600 spectrometer. Solid-state cross-polarization magic angle spinning (CP-MAS) ^{13}C NMR spectra were obtained on an Agilent Technologies DD2 400 spectrometer. Chemical shifts were expressed in part per million (ppm) with reference to the residual peaks of residual DMSO for ^1H (2.49 ppm) and ^{13}C (39.52 ppm). Gas sorption was measured by Micromeritics 3Flex and samples were loaded and degassed at 160°C for 3 h then at room temperature overnight before measurement. N_2 (99.99995%) sorption was measured at 77 K and CO_2 isotherms were recorded at 273 K and 298 K. The specific surface area was calculated according to Brunauer-Emmett-Teller (BET) theory. The pore size distribution was determined according to Barret-Joyner-Halenda (BJH) theory and the non-local density function theory (NLDFT) model with 77 K carbon slit pore model.

Synthesis of melamine-formaldehyde polymer particles. Inverse suspension polymerization was employed to synthesize the spherical particles. Oil phase was prepared in a 50 mL of a round-bottomed flask as the suspension stabilizer Span® 80 (0.072 g; 3.0 wt % of the monomers) was dissolved in cyclohexane (19.2 mL; 4 times of water) and heated to 60°C with vigorous agitation. Melamine and paraformaldehyde (total 2.400 g; for **MF-DMSO-170**, 1.505 g of melamine and 0.896 g of paraformaldehyde used) were added in deionized water and sodium hydroxide (~0.020 g) was added as a basic catalyst to maintain pH 8-9. The mixture was heated at 60°C for 20 min until the solution became transparent. After the solution was allowed to cool, concentrated hydrochloric acid (1.0 mL) was added to change the pH to 1-2 and the solution was reheated to 60°C for 10 min. Then, the aqueous solution was suspended into the cyclohexane solution. The reaction was allowed at 1200 rpm of stirring and carried out at 60°C for 3 h. After polymerization, transparent white spherical particles were produced and these particles were filtered and washed several times with water and acetone.

Synthesis of melamine-formaldehyde polyHIPE monoliths. As an outer oil phase, 16 mL of toluene was prepared in a 70 mL of cylindrical vial. g of the suspension stabilizer Tween 20 (10 wt/v % of total monomers) was dissolved in toluene and heated it to 60°C with vigorous agitation. Prior to reaction of aqueous phase, melamine (1.970 g, 16 mmol) and formaldehyde (1.407 g, 47 mmol) were dissolved in 4.8 mL of water (70 wt/v% of the monomers) in a 50 mL of a round-bottomed flask. Sodium hydroxide (~0.040 g) was added as a basic catalyst to maintain pH 8-9. The mixture was heated at 80°C for 5 min until the solution became transparent. After the solution was allowed to cool to 40°C, concentrated hydrochloric acid (1.0 mL) was added and the solution was reheated to 60°C for 5 min. A viscous polymer solution was obtained and it was poured into the toluene solution and sonicated for 5 min for emulsifying. The solution was heated at 60°C for 24 h with 1200 rpm of stirring. After polymerization, white bulky products were produced and soaked in deionized water overnight. The product was washed several times with water and acetone.

Synthesis of N^2,$N^{2'}$-(ethane-1,2-diyl)bis(1,3,5-triazine-2,4,6-triamine) (M1). To a round-bottomed flask equipped with a reflux condenser, ethylene diamine (0.34 mL, 5 mmol), 6-chloro-1,3,5-triazine-2,4-diamine (1.445 g, 10 mmol), triethylamine (1.40 mL, 10 mmol) and 50 mL of water were added and heated at 110°C overnight. The mixture was poured into an ice water and resulting white precipitations were filtered and rinsed with water several times, and dried in a vacuum oven at 40°C. ^{1}H NMR (600 MHz, DMSO-d_6, ppm): 6.36 (t, J = 5.4 Hz, 2H), 6.09-5.94 (m, 8H), 3.28 (t, 4H). ^{13}C NMR (151 MHz, DMSO-d_6, ppm): 167.07, 166.48, 40.05.

Synthesis of 6,6'-(piperazine-1,4-diyl)bis(1,3,5-triazine-2,4-diamine) (M2). To a round-bottomed flask equipped with a reflux condenser, piperazine (0.431 g, 5 mmol), 6-chloro-1,3,5-triazine-2,4-diamine (1.445 g, 10 mmol), sodium hydroxide (0.800 g, 20 mmol) and 50 mL of water were added and heated at 110°C for 2 d. The mixture was allowed to cool until white precipitations were formed. The white precipitations were filtered and rinsed with water several times, and dried in a vacuum oven at 40°C. ^{1}H NMR (600 MHz, DMSO-d_6, ppm): 6.14 (s, 8H), 3.63 (s, 8H). ^{13}C NMR (151 MHz, DMSO-d_6, ppm): 167.20, 165.38, 42.38.

Synthesis of dimelamine-formaldehyde polymer particles. Inverse suspension polymerization using prepolymer aqueous solution, cyclohexane and Span® 80 was performed as the previous way, whereas **M1** or **M2** was used instead of melamine monomer. **M1** (2.347 g) or **M2** (2.409 g), formaldehyde solution (2.5 mL for **M1F** and 2.4 mL for **M2F**), 1.0 mL of concentrated hydrochloric acid and 1.3 mL of water were mixed and heated at 70°C for 20 min. When the solution became transparent, it was suspended into the cyclohexane solution (above-mentioned oil phase). The reaction was allowed at 1200 rpm of stirring and carried out at 60°C for 3 h. After polymerization, transparent white spherical particles were produced and these particles were filtered and washed several times with water and acetone.

Solvent-assisted curing of polymers. The prepared nonporous polymer products were added in 20 mL of a selected aprotic solvent in a 50 mL of round flask equipped with a mechanical stirrer and a reflux condenser. The equipped flask was heated in an oil bath at specified temperature with stirring for 24 h. The cured particles were filtered, washed with sodium hydroxide aqueous solution (0.1 M), water and acetone several times, and dried overnight in a vacuum oven at 120 or 160°C.

Selectivity study. To predict the efficacy of **MF-P** for CO_2 over N_2 separation, we employed ideal adsorbed solution theory (IAST) to determine the molar loadings in the binary mixture for specified partial pressures. In this study, the single-component isotherms of CO_2 and N_2 at 273 K and 298 K were fitted by dual-site Toth model that is expressed as

$$q = q_{CO_2} + q_{N_2} = \frac{q_{sat,CO_2} b_{CO_2} p}{\left[1 + (b_{CO_2} p)^t\right]^{1/t}} + \frac{q_{sat,N_2} b_{N_2} p}{\left[1 + (b_{N_2} p)^t\right]^{1/t}}$$

where q is amount of adsorbed gas, q_{sat} is the saturation amount of absorbed gas, p is gas phase pressure, b is the absorption affinity parameter, and t is the Toth constant. Parameters of the above expression were obtained by nonlinear regression of the experimental data by OriginPro 2019 software, as shown in Fig. S17 and supplementary table 2. IAST equation was calculated with the aid of MATLAB provided from https://github.com/KaihangShi. The adsorption selectivity for binary mixtures is defined by $S = \frac{q_{CO_2}/q_{N_2}}{p_{CO_2}/p_{N_2}}$ where q is the uptake amount and p is the partial pressure of each gas.

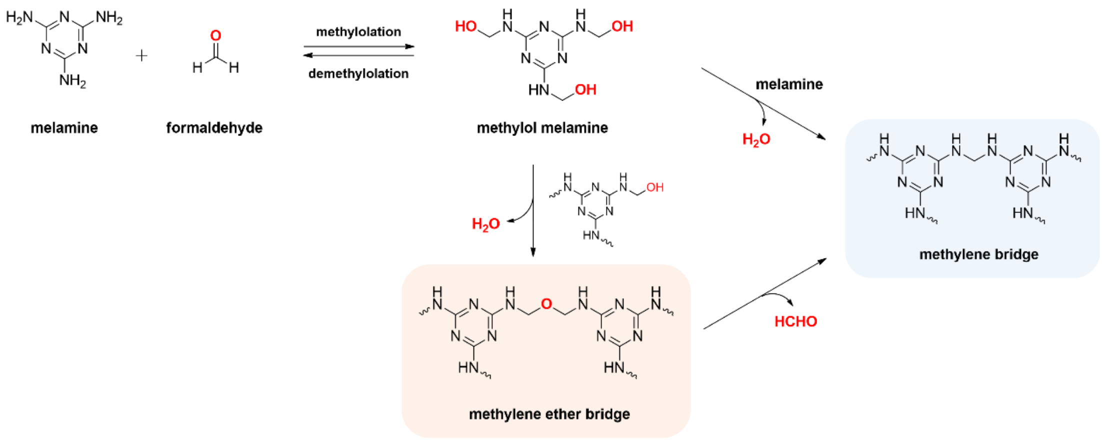

Figure S1 Synthetic route of methylene ether and methylene bridge.

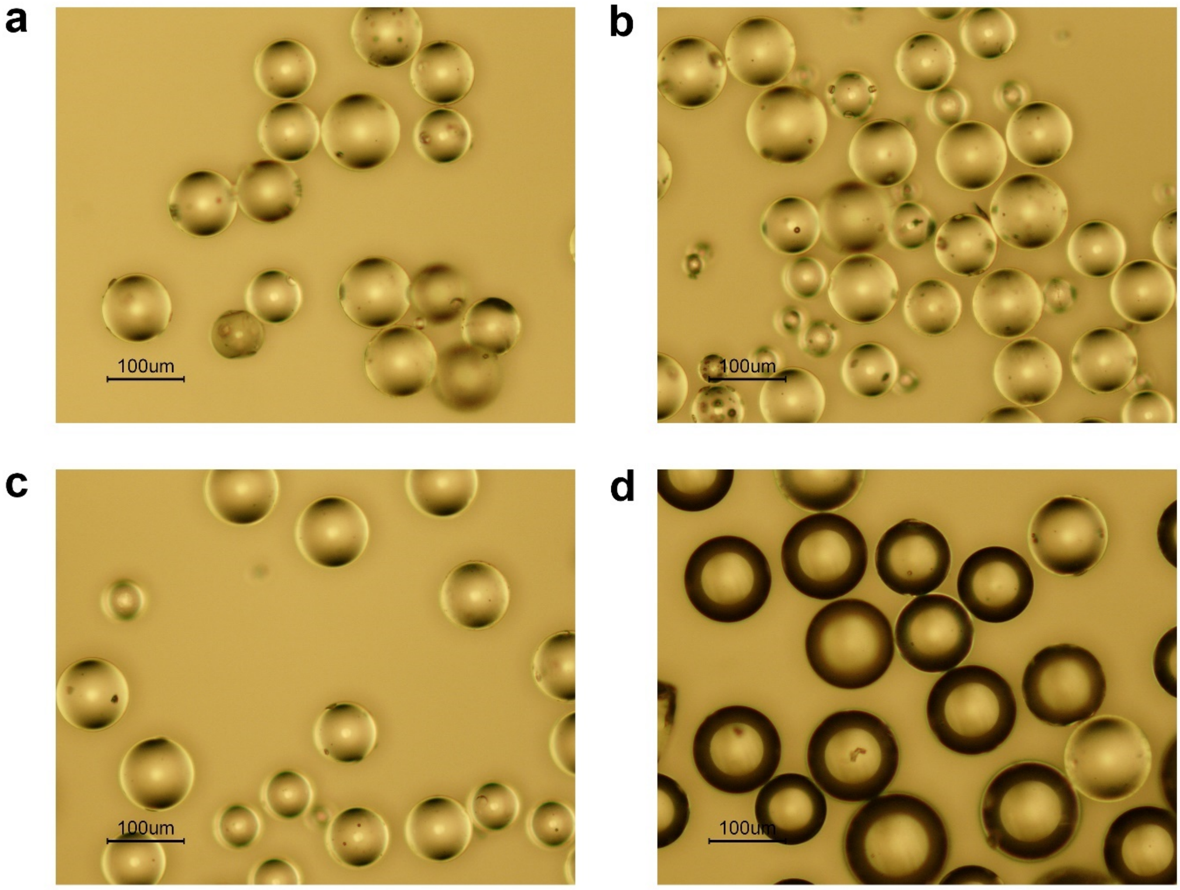

Figure S2 Optical microscopic images for **MF-P** particles cured in DMSO at 170°C for: **(a) 1 h**, **(b) 3 h**, **(c) 6 h**, and **(d) 12 h**.

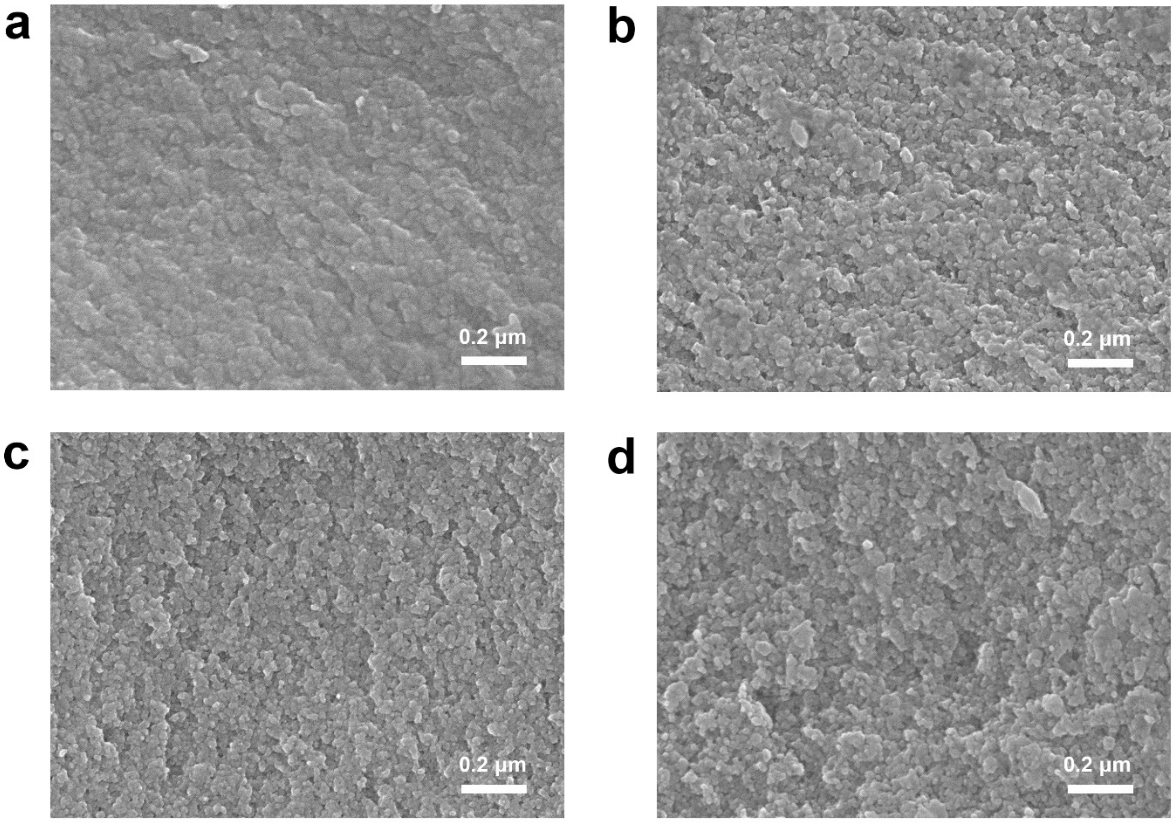

Figure S3 SEM images for **MF-P** particles cured in DMSO at 170°C for: **(a) 1 h**, **(b) 3 h**, **(c) 6 h**, and **(d) 12 h**.

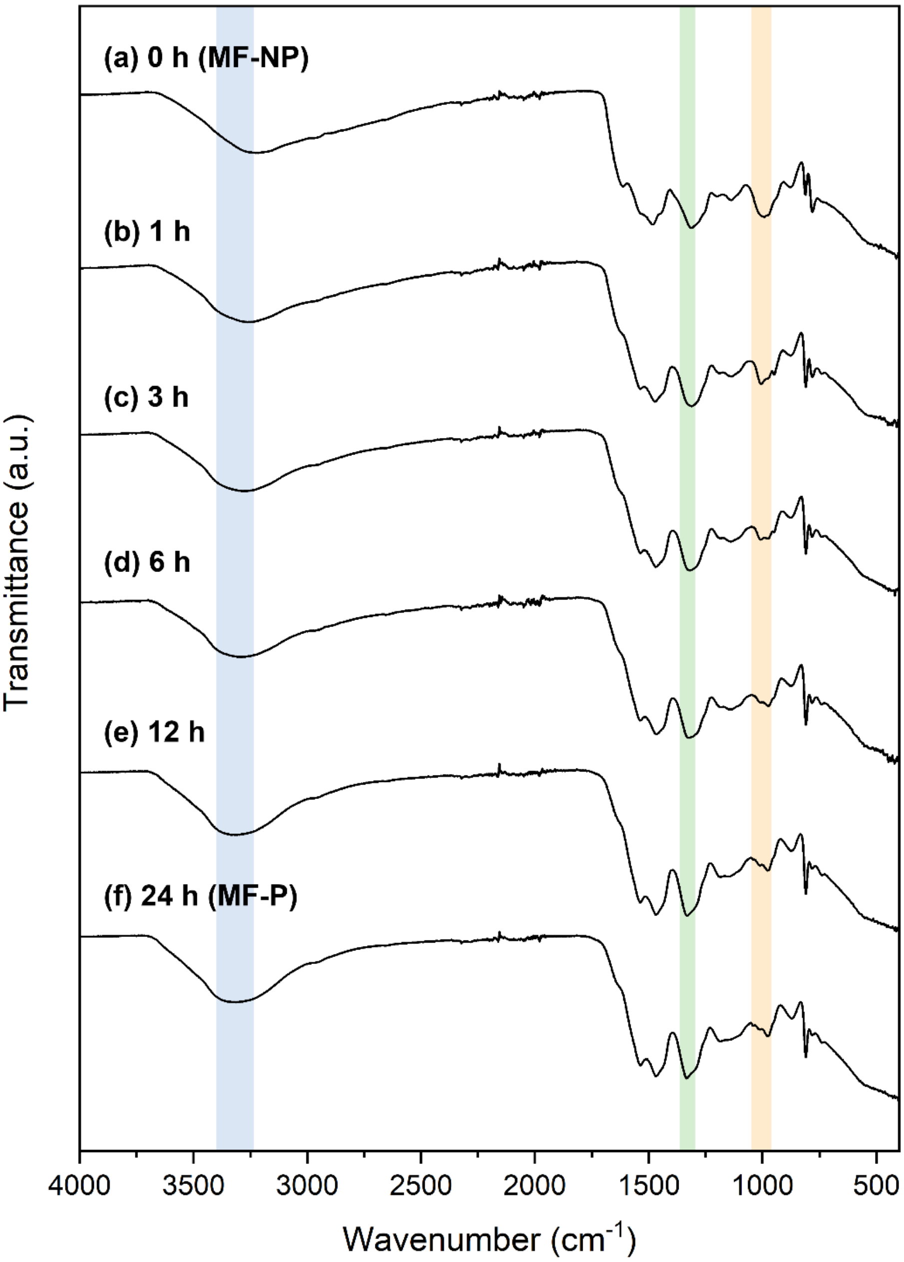

Figure S4 FT-IR spectra of **MF-NP** particles **(a)** uncured and cured in DMSO at 170°C for **(b) 1 h**, **(c) 3 h**, **(d) 6 h**, **(e) 12 h** and (f) **24 h** (**MF-P**).

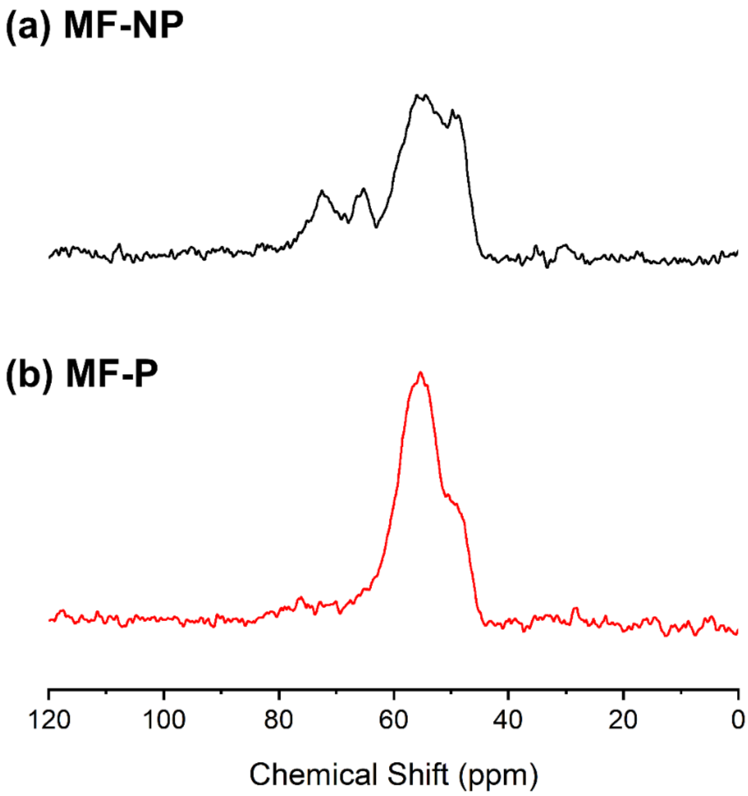

Figure S5 CP-MAS ^{13}C NMR spectra of **(a) MF-NP** and **(b) MF-P** particles (solid-state, 100MHz).

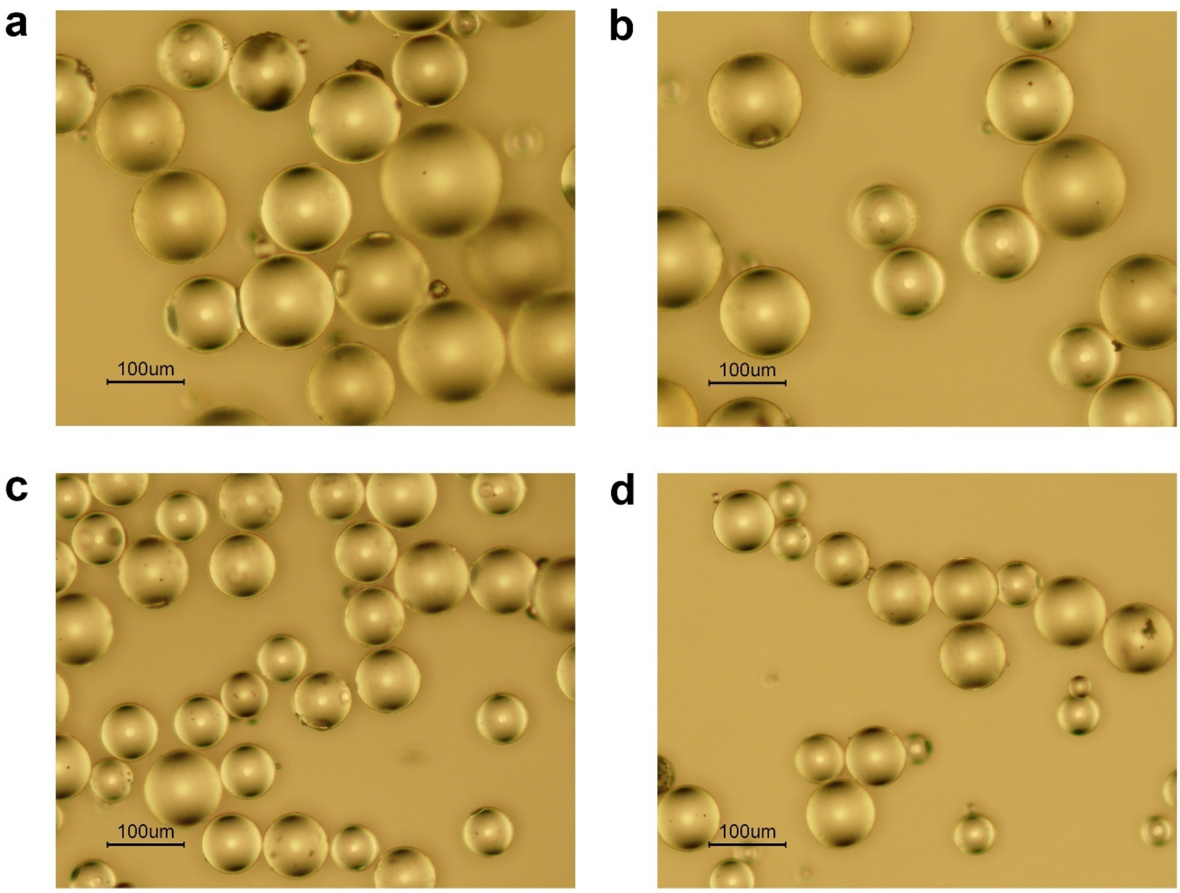

Figure S6 Optical microscopic images for **MF-NP** particles cured in oven for 24 h at: **(a)** 100°C, **(b)** 120°C, **(c)** 140°C, and **(d)** 170°C.

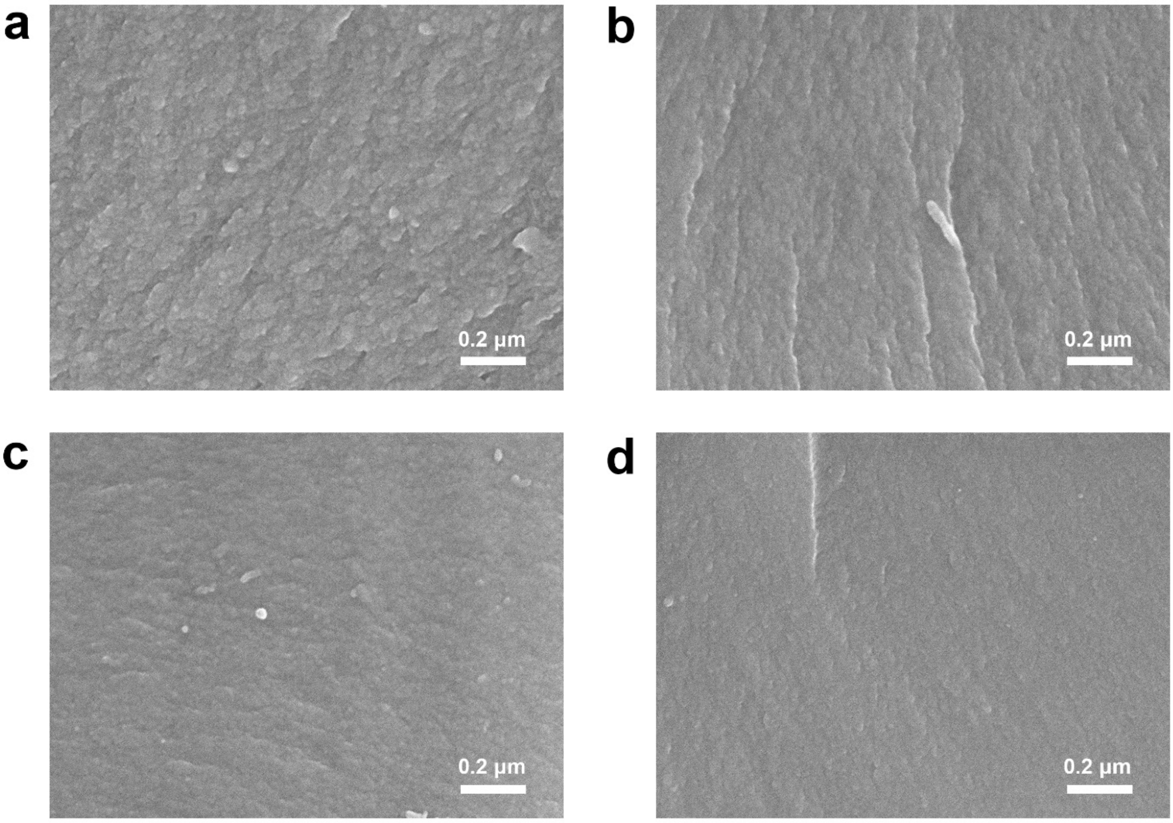

Figure S7 SEM images for **MF-NP** particles cured in oven for 24 h at: **(a)** 100°C, **(b)** 120°C, **(c)** 140°C, and **(d)** 170°C.

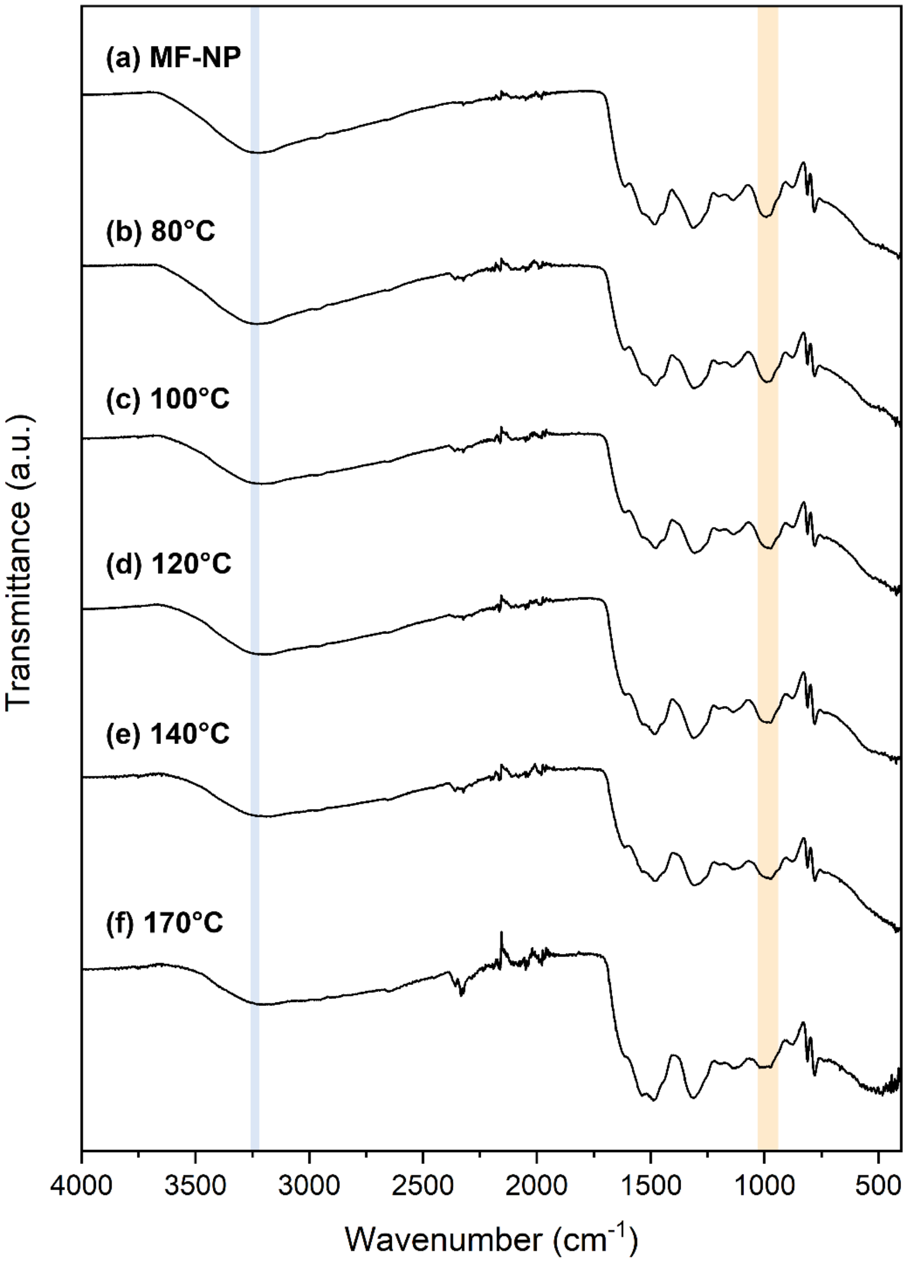

Figure S8 FT-IR spectra of **MF-NP** particles **(a)** uncured and cured in oven for 24 h at: **(b)** 80°C, **(c)** 100°C, **(d)** 120°C, **(e)** 140°C, and **(f)** 170°C.

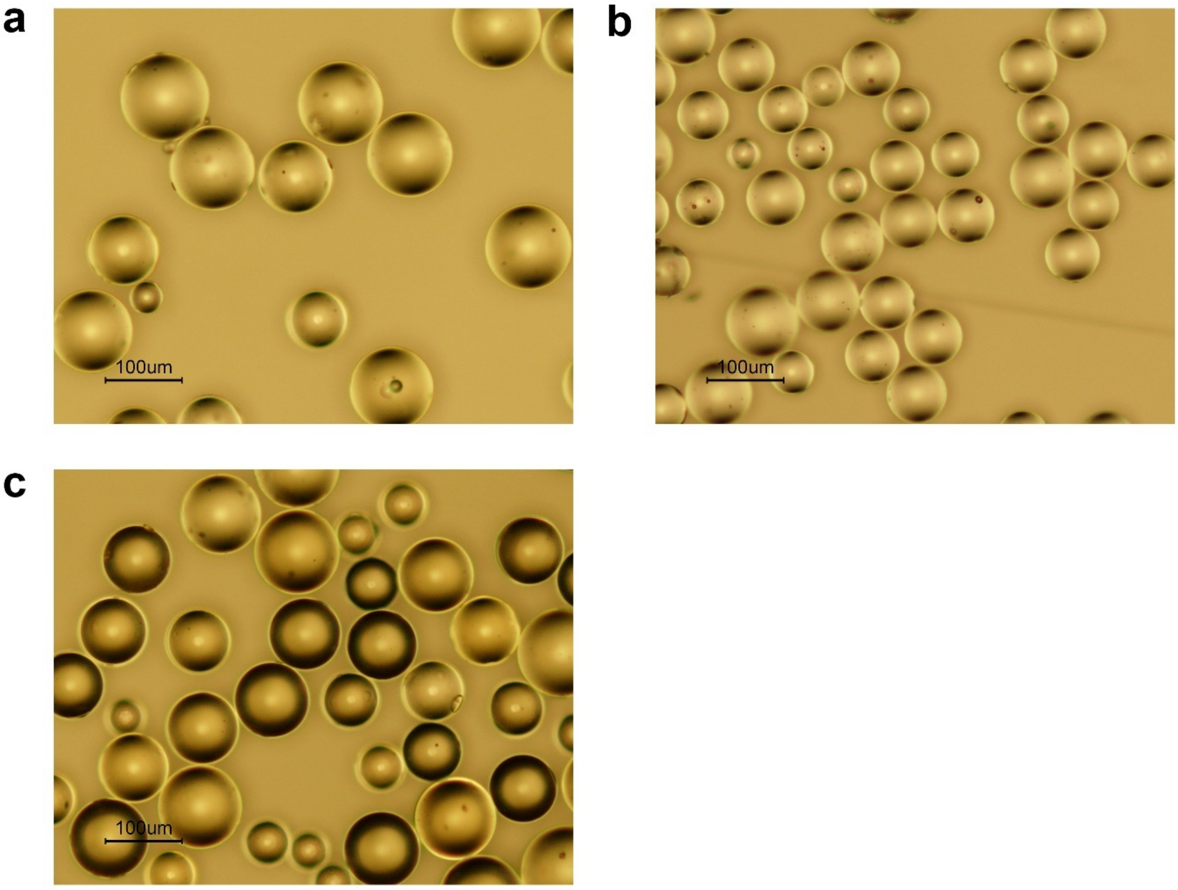

Figure S9 Optical microscopic images for **MF-NP** particles cured in DMSO for 24 h at: **(a)** 100°C, **(b)** 120°C, and **(c)** 140°C.

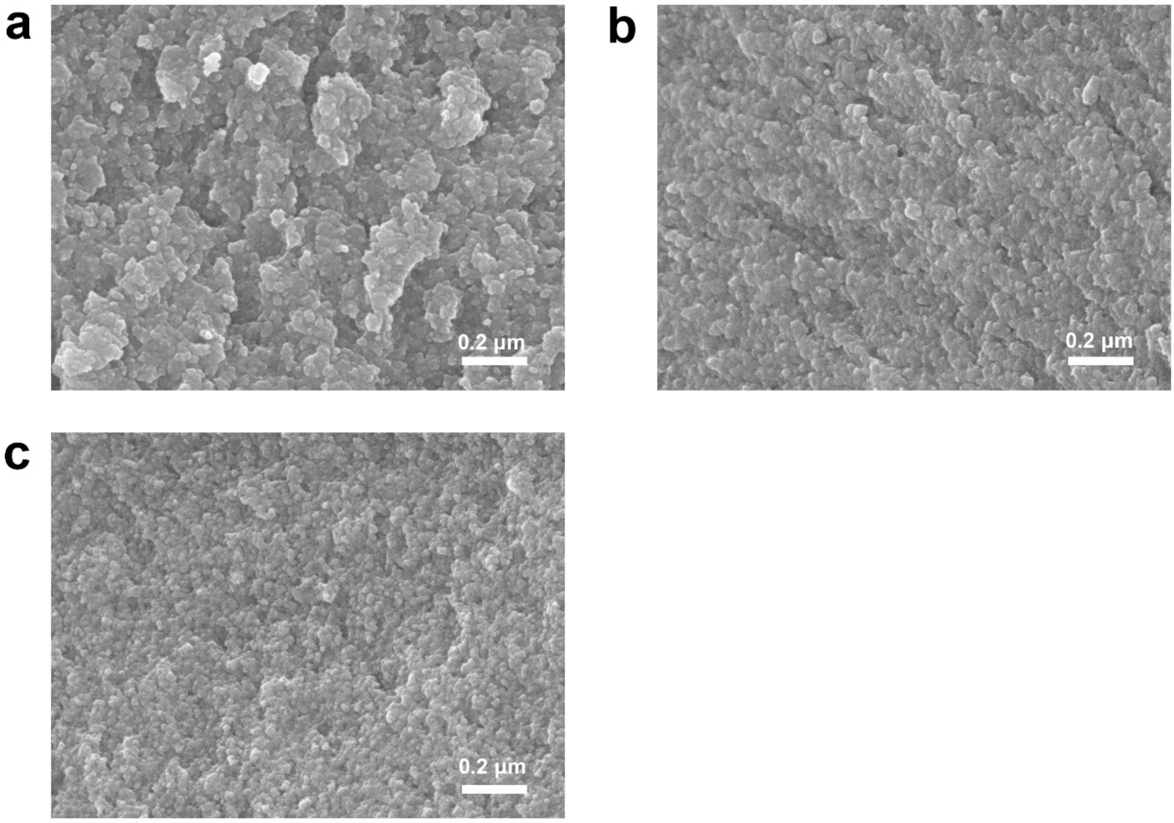

Figure S10 SEM images for **MF-NP** particles cured in DMSO for 24 h at: **(a)** 100°C, **(b)** 120°C, and **(c)** 140°C.

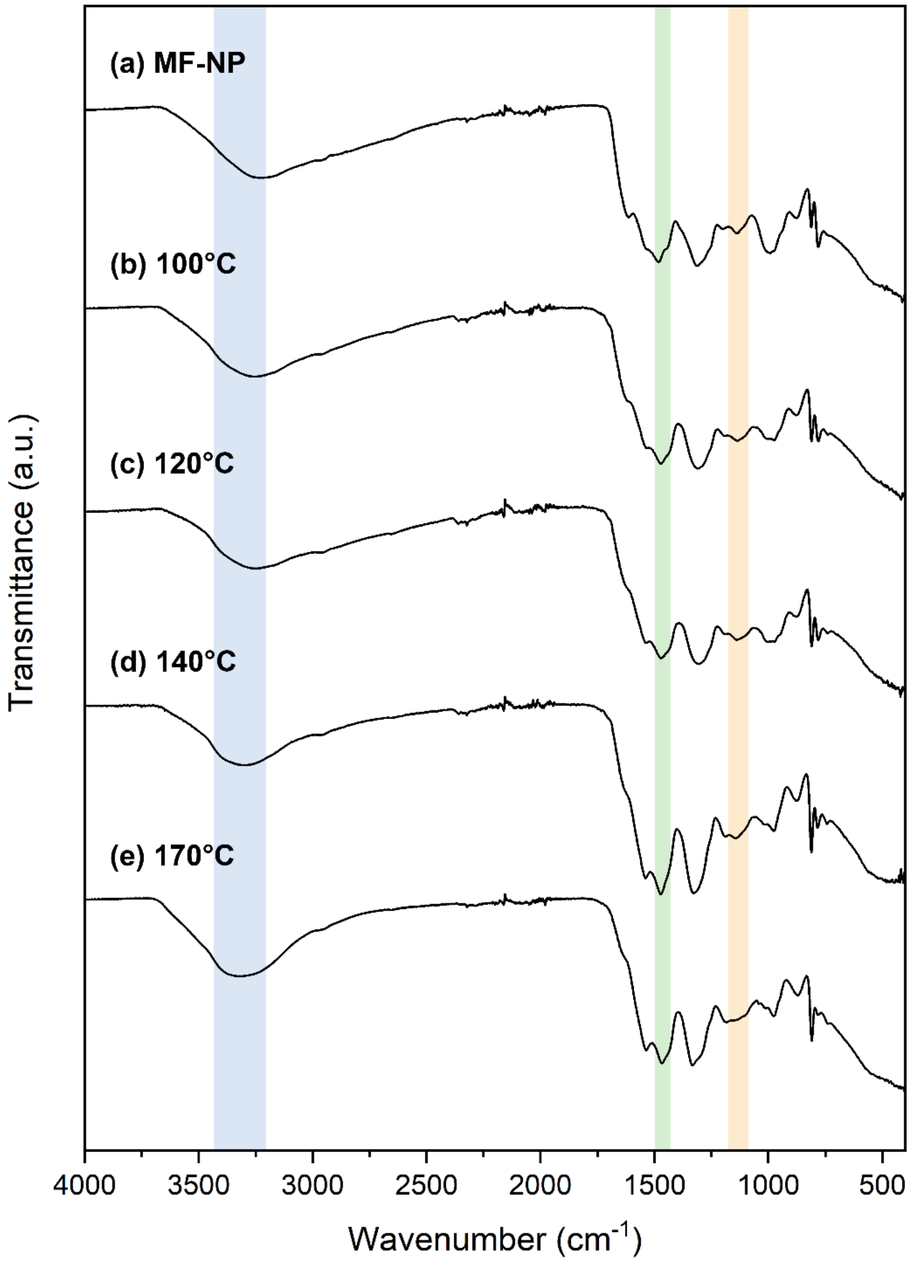

Figure S11 FT-IR spectra of **MF-NP** particles **(a)** uncured and cured in DMSO for 24 h at: **(b)** 100°C, **(c)** 120°C and **(d)** 140°C, and **(e)** 170°C (**MF-P**).

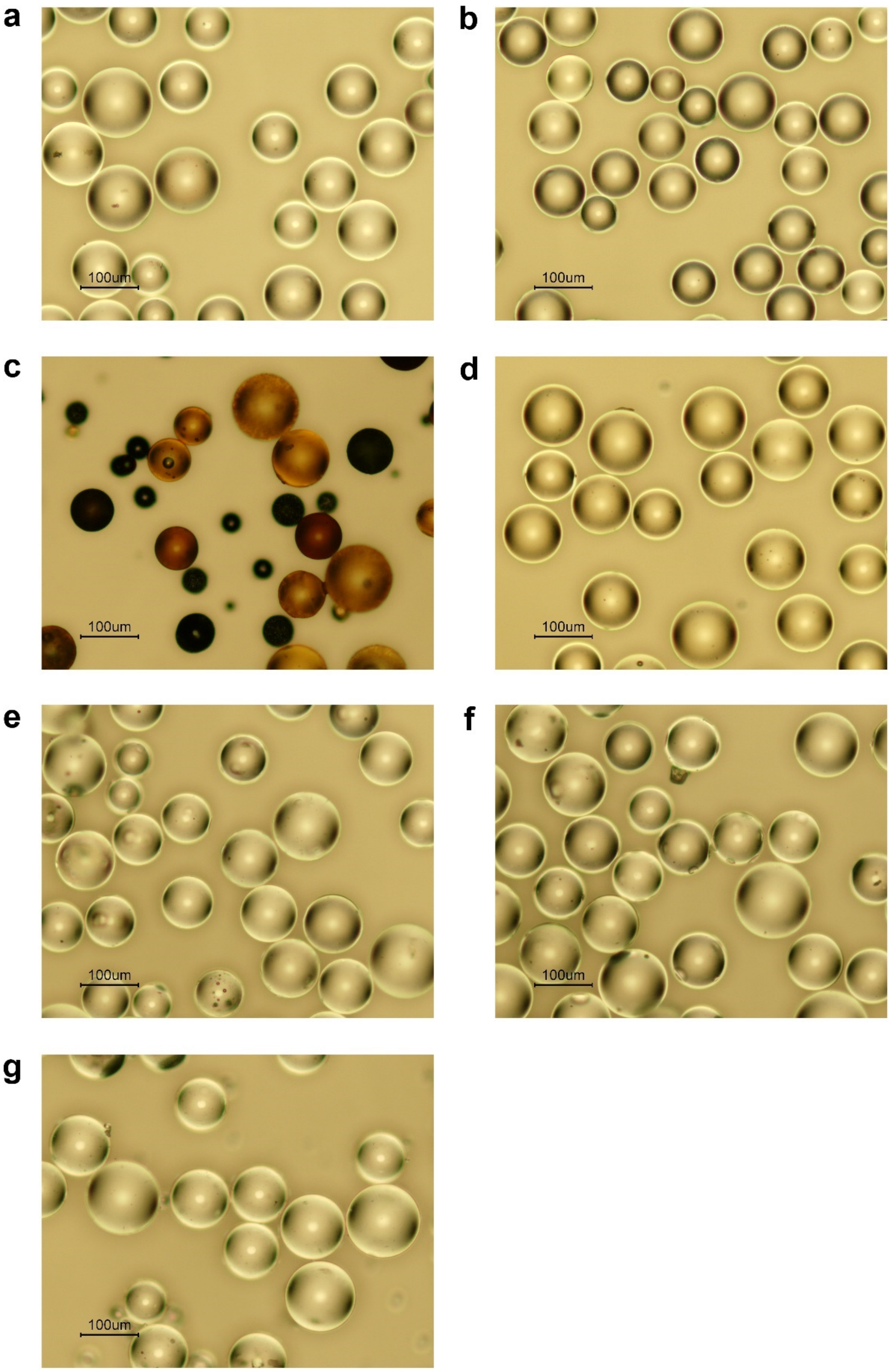

Figure S12 Optical microscopic images for various solvent curing: **(a) MF-DMAc-140**, **(b) MF-DMF-140**, **(c) MF-NMP-170**, **(d) MF-sulfolane-170**, **(e) MF-EA-70**, **(f) MF-THF-60** and **(g) MF-acetonitrile-65**.

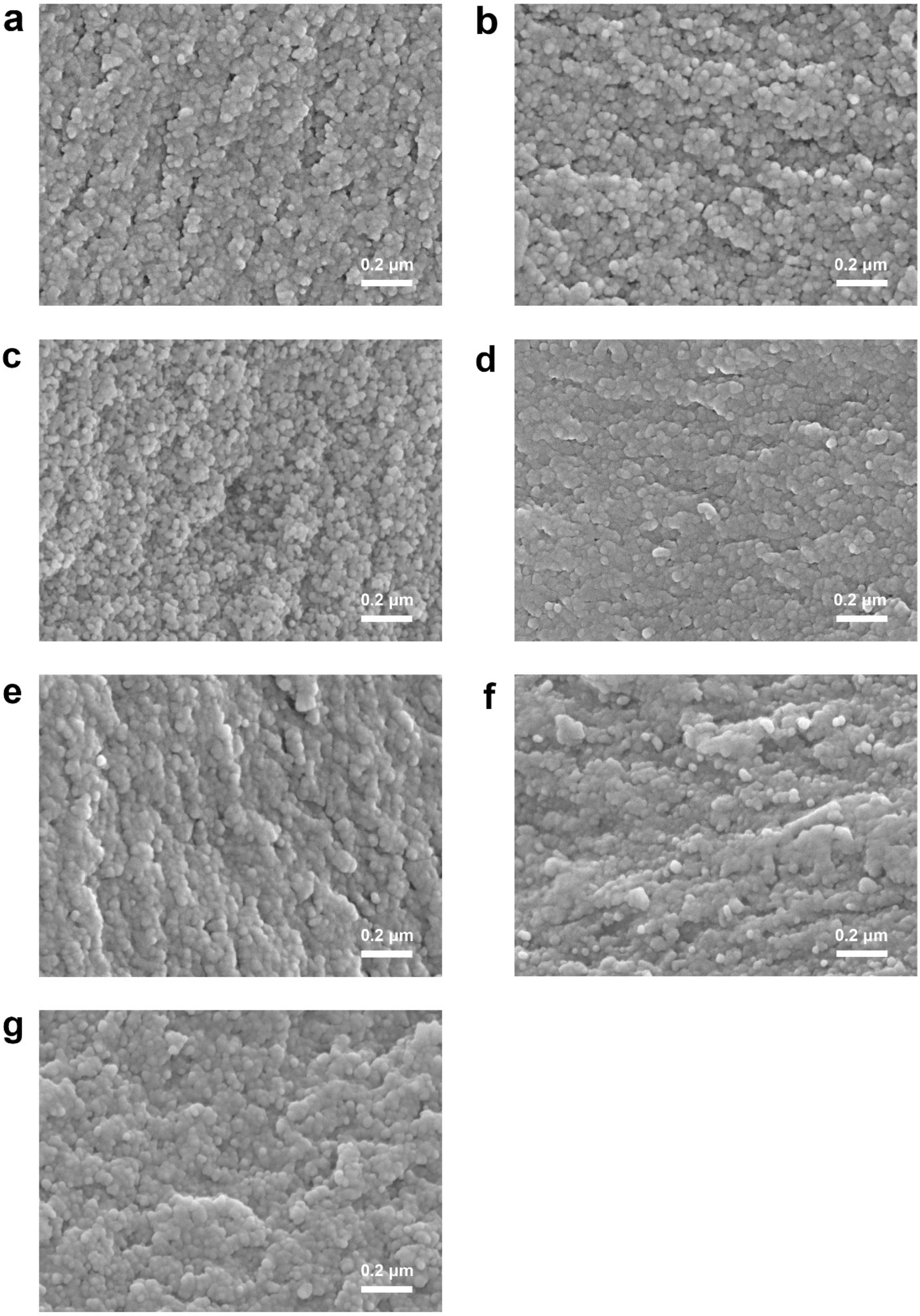

Figure S13 SEM images for various solvent curing: **(a) MF-DMAc-140**, **(b) MF-DMF-140**, **(c) MF-NMP-170**, **(d) MF-sulfolane-170**, **(e) MF-EA-70**, **(f) MF-THF-60** and **(g) MF-acetonitrile-65**.

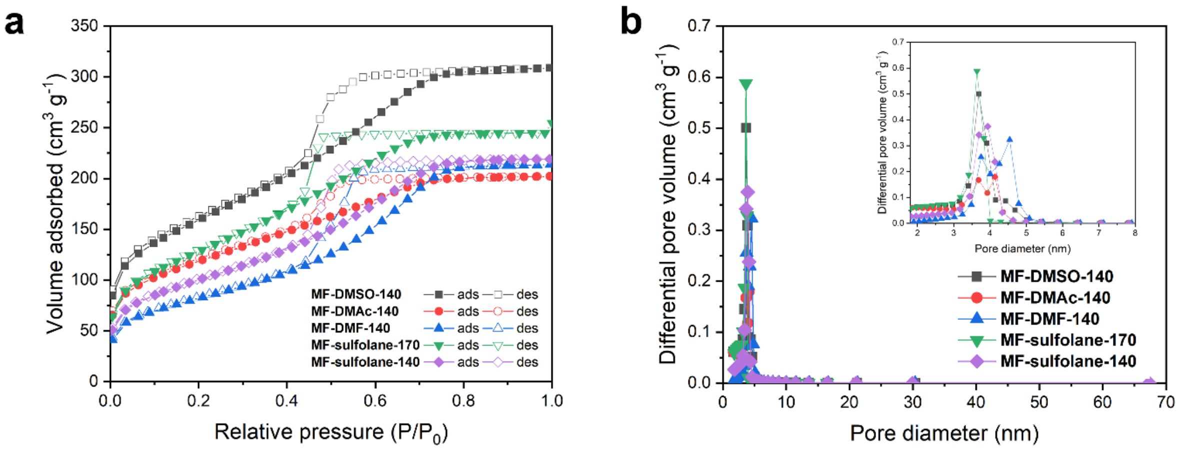

Figure S14 Physical characteristics of porous **MF-P** particles with various solvents in Table 1. **(a)** N_2 sorption isotherm and **(b)** pore size distribution.

Table S1 Physical properties of polar aprotic solvents. This data was obtained from U. Tilstam, *Org. Process Res. Dev*, **2012**, *16*, 1273.

Property	DMSO	DMAc	DMF	NMP	Sulfolane
Relative molecular mass	78.13	87.12	73.09	99.13	120.17
Density (g·cm^3)	1.10	0.94	0.94	1.03	1.26
Boiling point (°C)	189.1	166.2	153.1	201.9	287.3
Melting point (°C)	18.6	-20.1	-60.4	-24.4	28.4
Relative permittivity (ε_υ)	46.7 @25°C	37.8 @25°C	36.7 @25°C	32.2 @25°C	43.4 @30°C

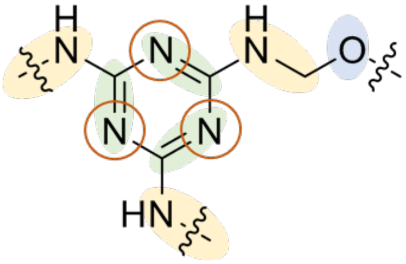

Figure S15 Repeating unit of **MF-NP**.

Table S2 Calculation of Hansen solubility parameters for **MF-NP** considering functional groups.

	Functional group	δ_d	δ_p	δ_h	Occurrences
Primary	>C=N– (green)	-0.3074	-0.0012	-5.3956	3
	CH_2NH (yellow)	0.8116	0.9412	1.3400	3
	–O– (blue)	0.0472	3.3432	0.0256	1
Secondary	>N{H or C} (in cyclic, red)	0.2218	-2.2018	-0.0452	3
Result for MF-NP		**19.5483**	**6.9126**	**-4.2975**	

Table S3 Hansen solubility parameter of curing solvents and calculated $\Delta\delta$ between solvent and **MF-NP**.

Solvent[a]	δ_d	δ_p	δ_h	$\Delta\delta$
DMSO	18.4	16.4	10.2	17.3640
DMAc	16.8	11.5	10.2	15.4523
DMF	17.4	13.7	11.3	17.1454
NMP	18.0	12.3	7.2	12.7912
Sulfolane	20.3	18.2	10.9	18.9456

[a] All parameters for solvents were excerpted from C. M. Hansen, Hansen Solubility Parameters: A User's Handbook, Second Edition (2000).

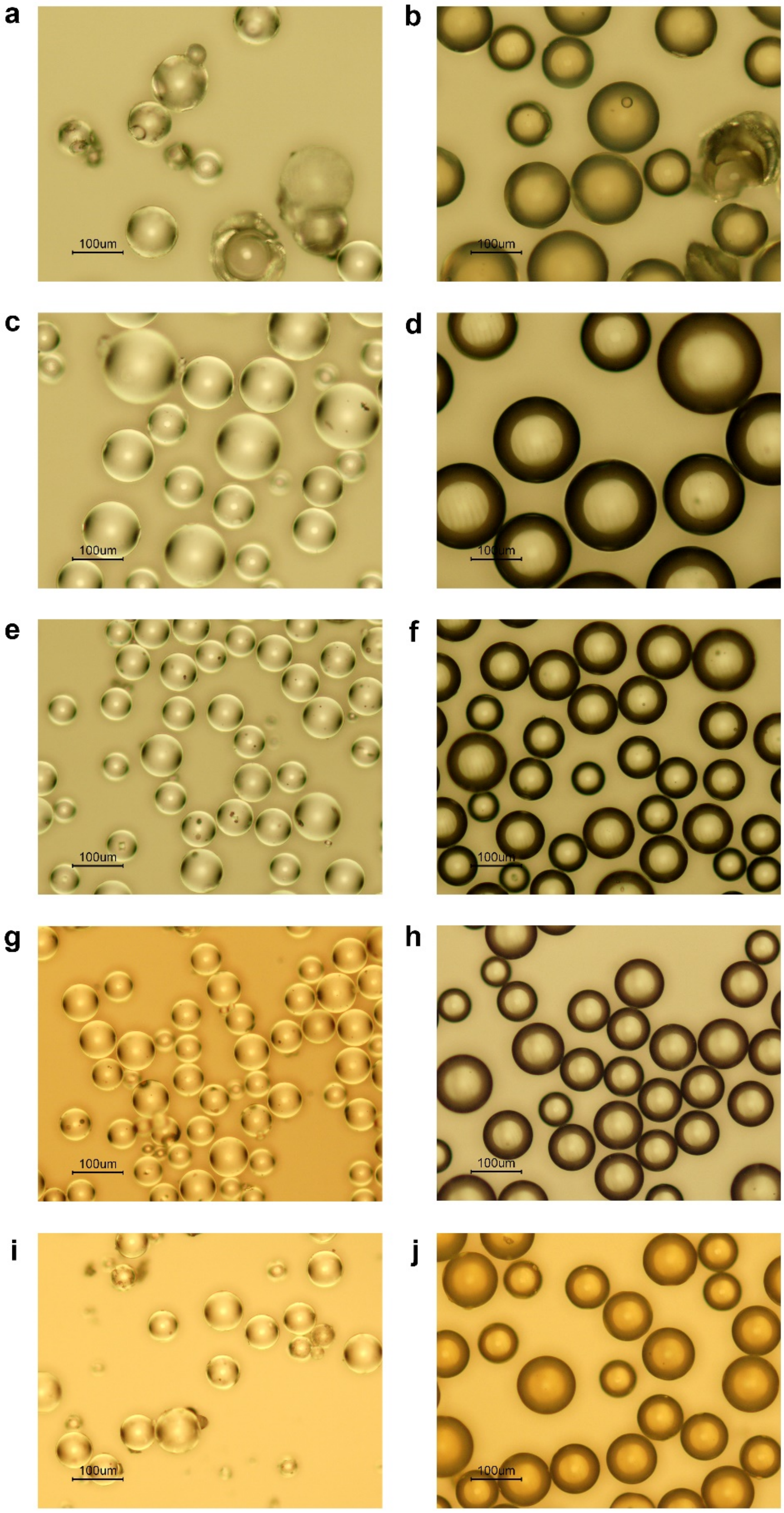

Figure S16 Optical microscopic images for various monomer ratios: **MF-DMSO-1.5 (a)** before curing and **(b)** after curing. **MF-DMSO-2.0 (c)** before curing and **(d)** after curing. **MF-DMSO-3.0 (e)** before curing and **(f)** after curing. **MF-DMSO-4.0 (g)** before curing and **(h)** after curing. **MF-DMSO-6.0 (i)** before curing and **(j)** after curing.

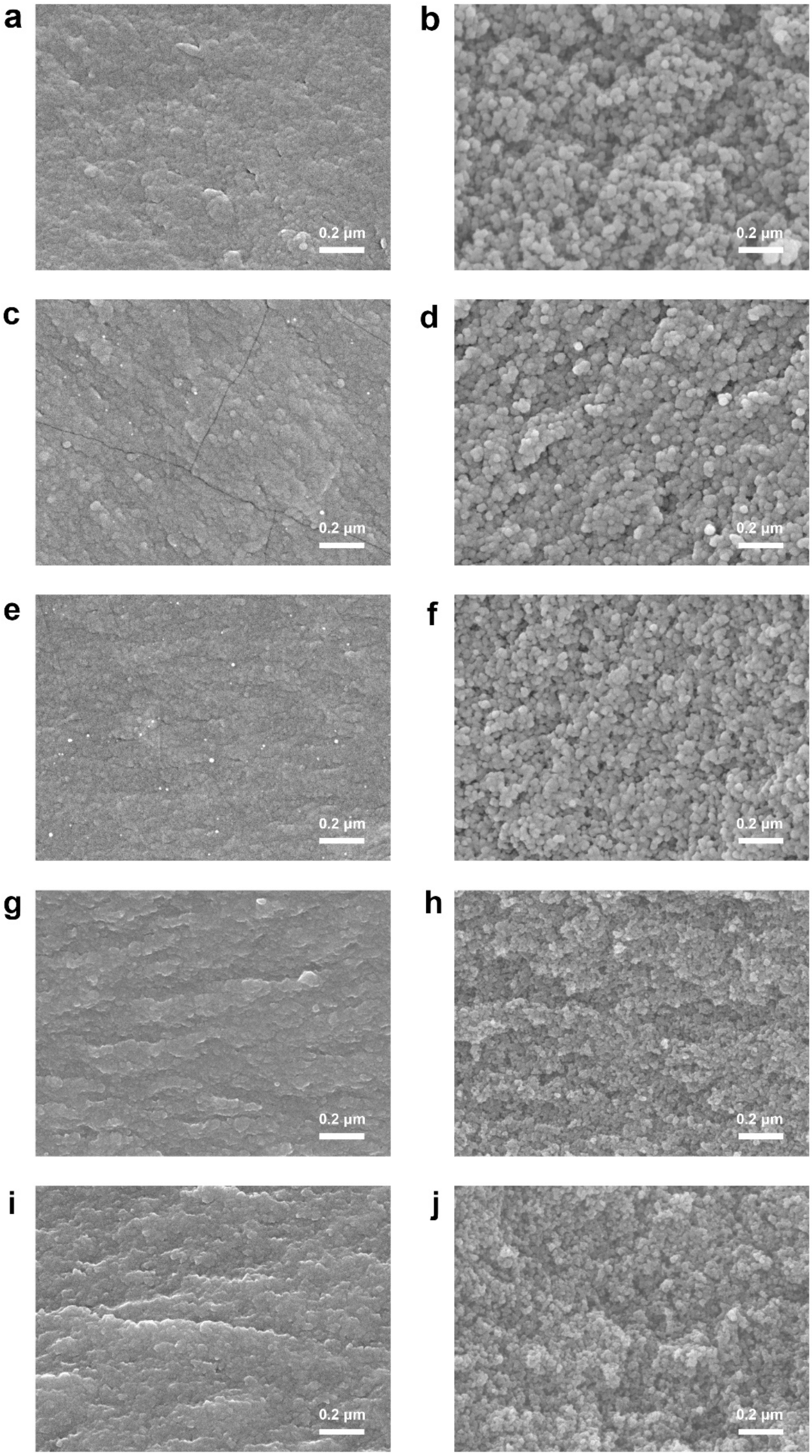

Figure S17 SEM images for various monomer ratios: **MF-DMSO-1.5 (a)** before curing and **(b)** after curing. **MF-DMSO-2.0 (c)** before curing and **(d)** after curing. **MF-DMSO-3.0 (e)** before curing and **(f)** after curing. **MF-DMSO-4.0 (g)** before curing and **(h)** after curing. **MF-DMSO-6.0 (i)** before curing and **(j)** after curing.

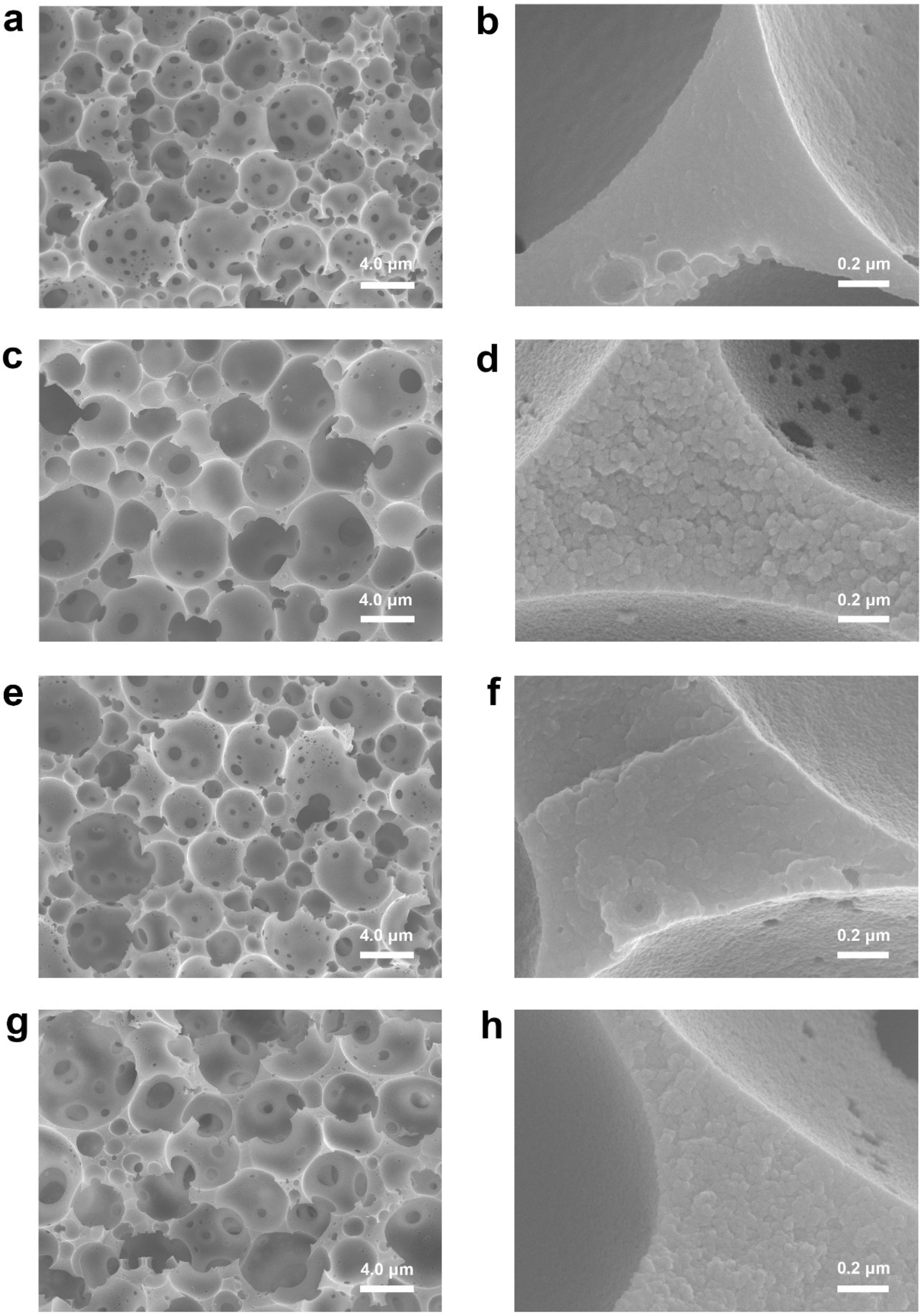

Figure S18 SEM images for **MF-P** polyHIPEs: **MF-HIPE-2.5 (a)**, **(b)** before curing and **(c)**, **(d)** after curing. **MF-HIPE-3.5 (e)**, **(f)** before curing and **(g)**, **(h)** after curing.

Table S4. Physical characteristics of **MF-P** polyHIPEs from N_2 sorption

Entry	F/M ratio[a]	S_{BET}[b] $[m^2\ g^{-1}]$	V_{total}[c] $[cm^3\ g^{-1}]$	V_{micro}[d] $[cm^3\ g^{-1}]$	Pore size[e] [nm]
MF-HIPE-2.5	2.5	464	0.79	0.023	6.68
MF-HIPE-3.0	3.0	600	0.79	0.052	5.56
MF-HIPE-3.5	3.5	545	0.70	0.027	5.17

[a] Paraformaldehyde/melamine molar ratio. [b] BET specific surface area. [c] Total pore volume at $P/P_0 \approx 0.99$. [d] Micropore volume calculated by T-plot equation. [e] Average pore diameter by BJH method.

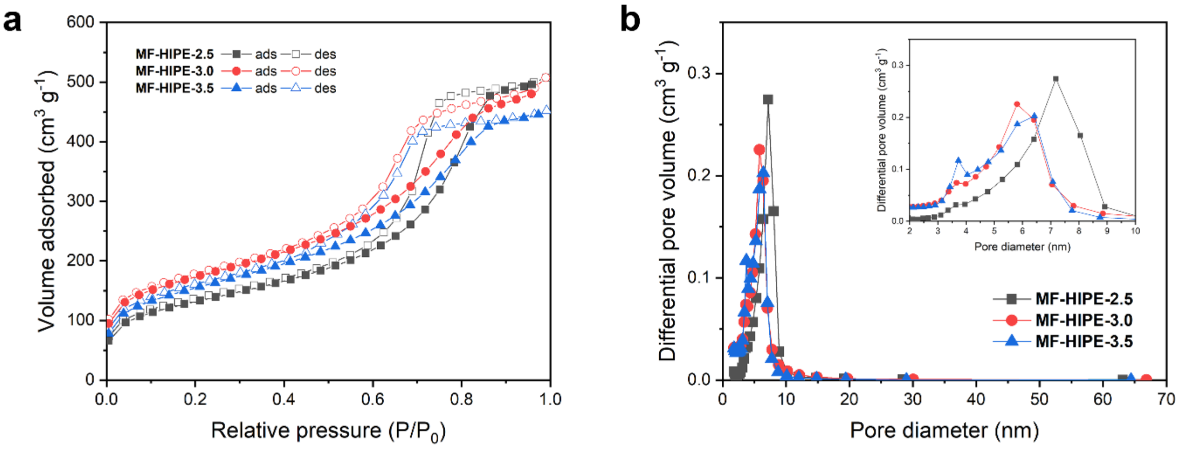

Figure S19 (a) N_2 sorption isotherms and **(b)** pore size distribution of **MF-P** polyHIPEs.

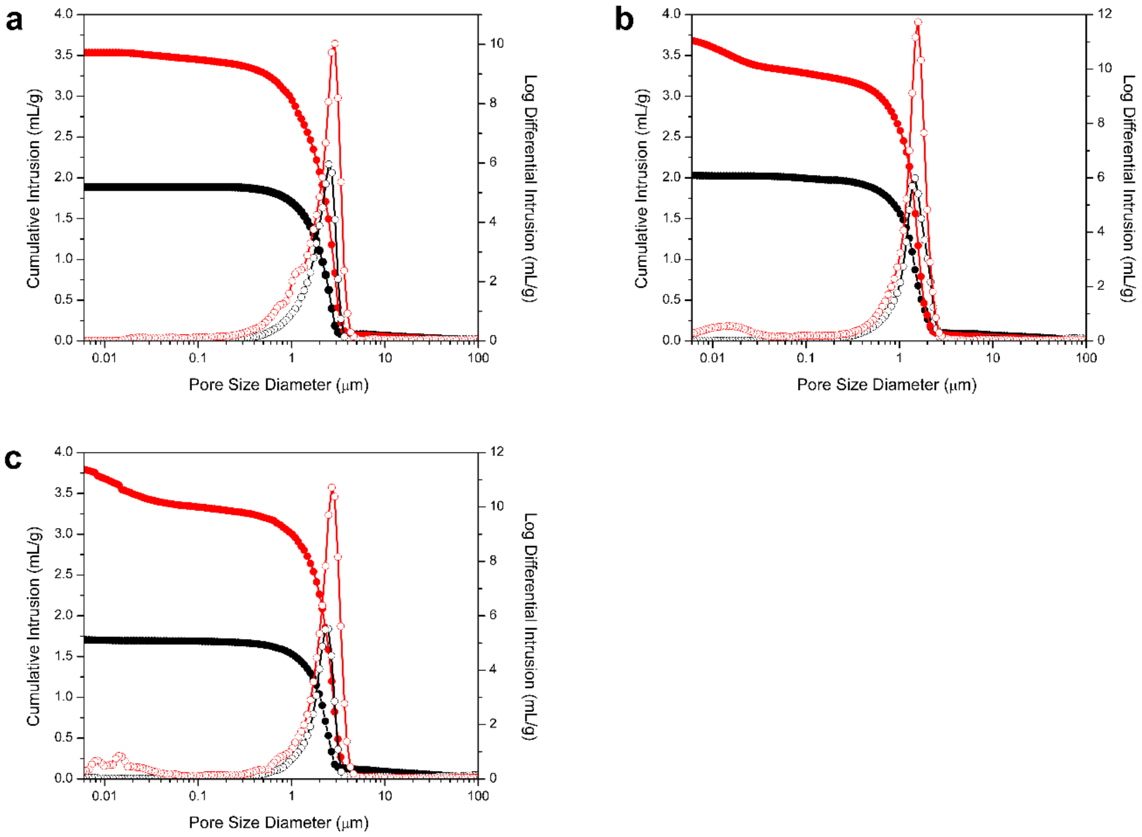

Figure S20 Hg intrusion isotherms and pore size distribution of **(a) MF-HIPE-2.5**, **(b) MF-HIPE-3.0** and **(c) MF-HIPE-3.5** before curing (black) and after curing (red).

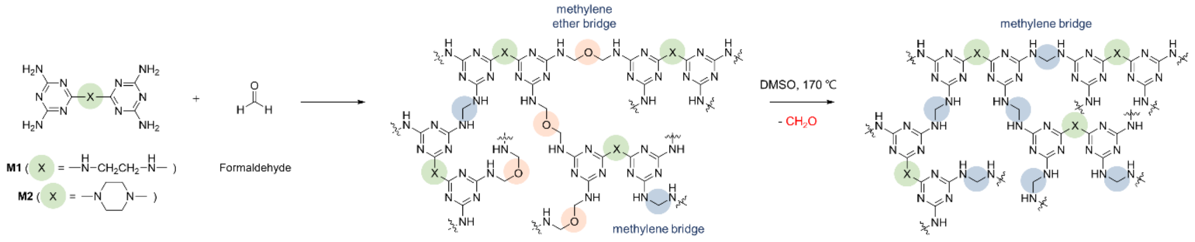

Figure S21 Synthetic route of **M1F** and **M2F** polymers.

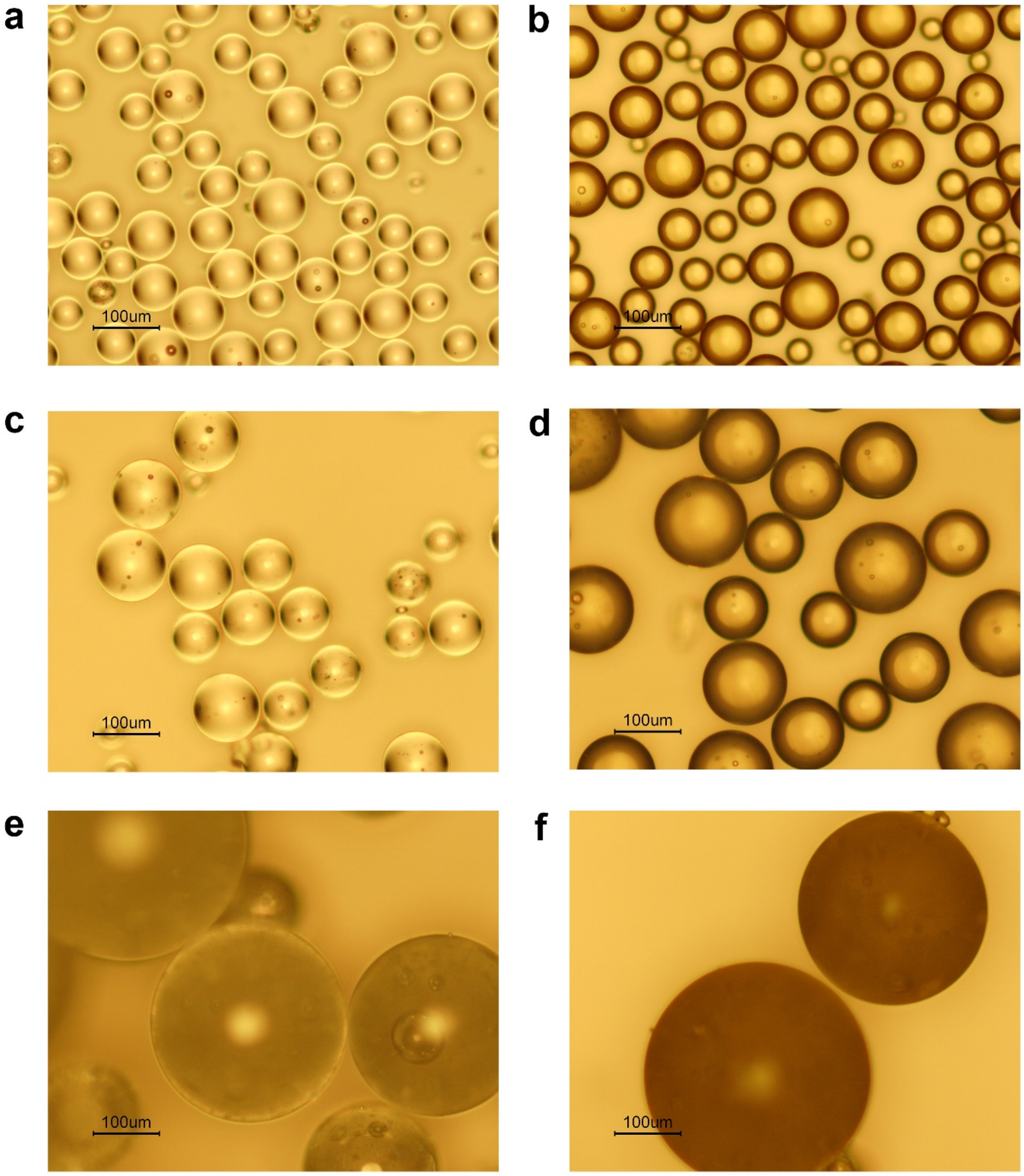

Figure S22 Optical microscopic images for various monomers: **(a) M0F-NP** and **(b) M0F-P** particles. **(c) M1F-NP** and **(d) M1F-P** particles. **(e) M2F-NP** and **(f) M2F-P** particles.

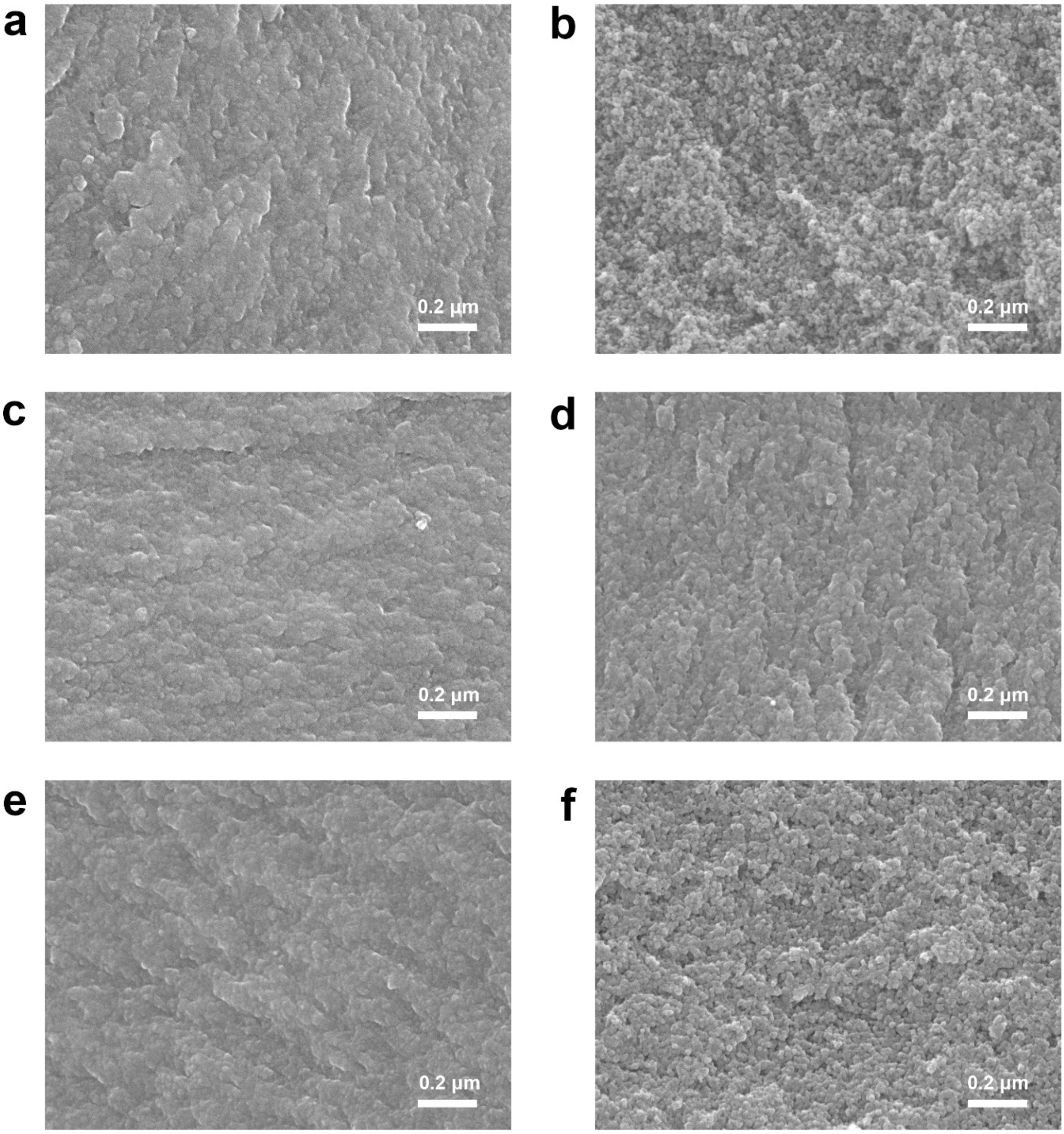

Figure S23 SEM images for monomers: **(a) M0F-NP** and **(b) M0F-P** particles. **(c) M1F-NP** and **(d) M1F-P** particles. **(e) M2F-NP** and **(f) M2F-P** particles.

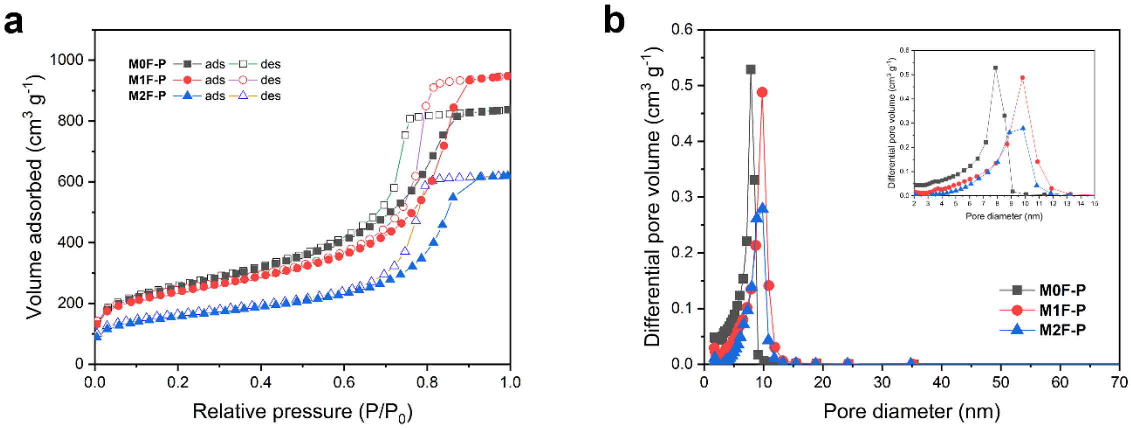

Figure S24 (a) N_2 sorption isotherms and **(b)** pore size distribution of **M0F-P**, **M1F-P** and **M2F-P**.

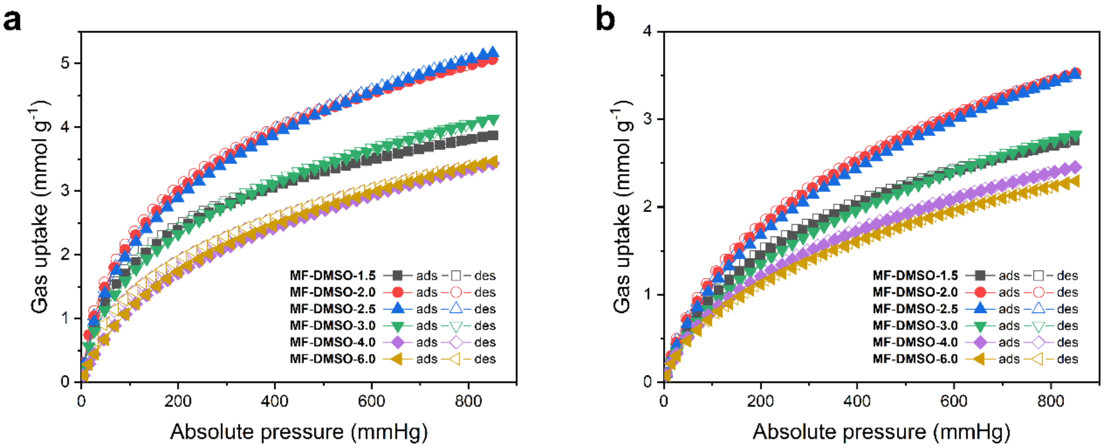

Figure S25 CO_2 sorption isotherms at **(a)** 273 K and **(b)** 298 K of **MF-P** particles

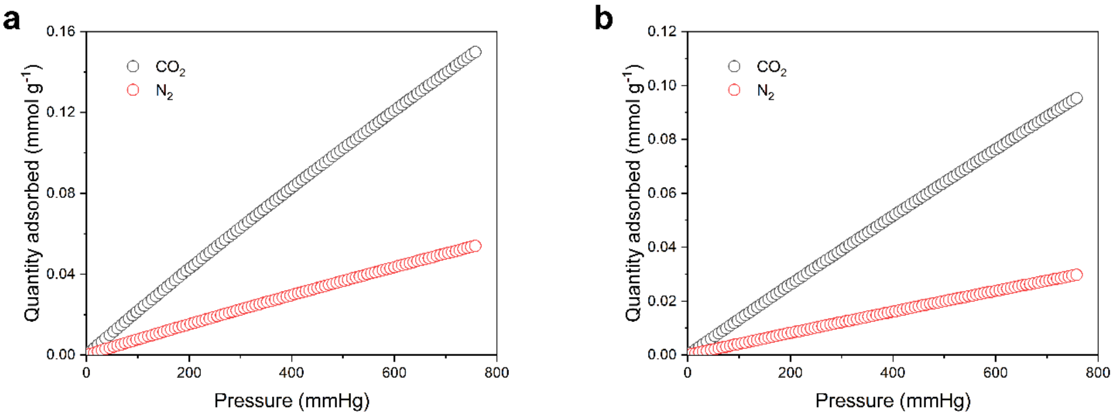

Figure S26 IAST binary adsorption isotherms for **MF-DMSO-170** at **(a)** 273 K and **(b)** 298 K with CO_2 and N_2 molar ratio of 15/85 in the gas phase.

Table S5 Toth fitting parameters of CO_2 and N_2 adsorption isotherms of **MF-DMSO-170** measured at 273K and 298 K.

Temperature	Gas	q_{sat} [mmol g^{-1}]	b [mmHg^{-1}]	t	R^2
273 K	CO_2	10.63968	0.00106	0.63751	0.99979
	N_2	2.27885	3.04131E-4	0.99709	0.99998
298 K	CO_2	8.00231	8.37929E-4	0.74645	0.99989
	N_2	1.73353	2.12261E-4	1.02988	0.99995

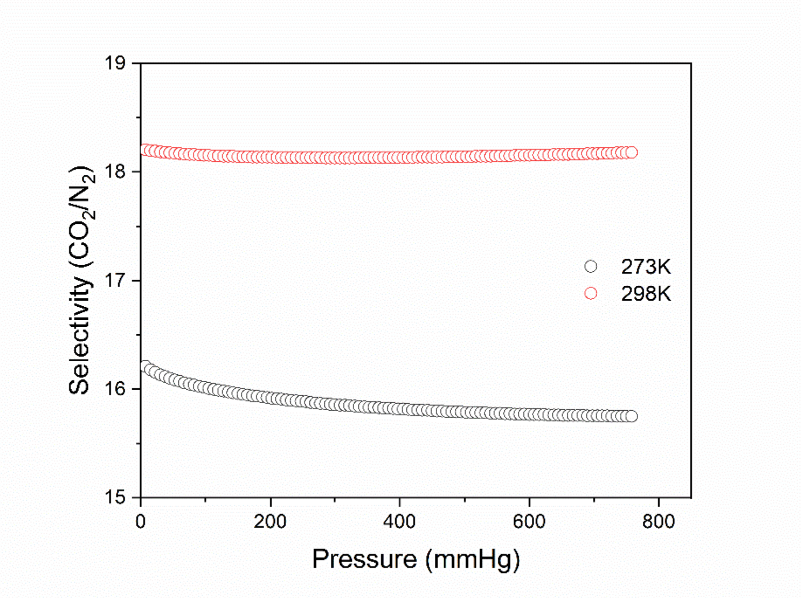

Figure S27 Calculated IAST adsorption selectivity of **MF-DMSO-170** at a 15/85 of CO_2/N_2 molar ratio.

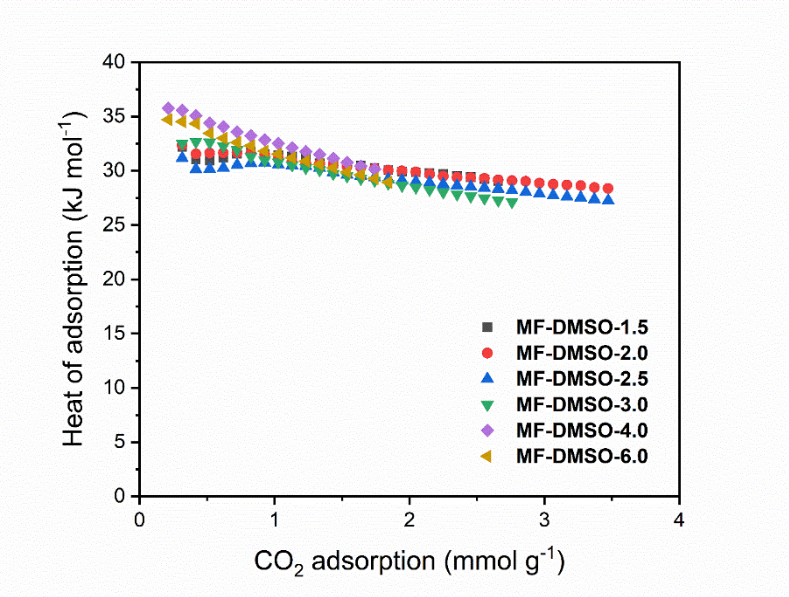

Figure S28 Heat of adsorption graph of **MF-P** particles.